Densification of Digital Terrain Elevations Using Shape from Shading with Single Satellite Imagery

Mohammad A. Rajabi [1], J. A. Rod Blais [1]

Dept. of Geomatics Eng., The University of Calgary, 2500, University Dr., NW, Calgary, Alberta, Canada, T2N 1N4

{marajabi, blais}@ucalgary.ca

Abstract. Numerous geoscience and engineering applications need denser and more accurate Digital Terrain Model (DTM) height data. Collecting additional height data in the field, if not impossible, is either expensive or time consuming or both. Stereo aerial or satellite imagery is often unavailable and very expensive to acquire. Interpolation techniques are fast and cheap, but have their own inherent difficulties and problems, especially in rough terrain. Advanced space technology has provided much single (if not stereo) high-resolution satellite imageries almost worldwide. This paper discusses the idea of using Shape From Shading (SFS) methods with single high resolution imagery to densify regular grids of heights. Preliminary results are very encouraging and the methodology is going to be implemented with real satellite imagery and parallel computations.

1 Introduction

In the present context, Digital Terrain Models (DTMs) are simply regular grids of elevation measurements over the land surface. They are used for the analysis of topographical features in GISs and numerous engineering computations. The National Center for Geographic Information and Analysis (NCGIA) provides a list of global DTMs with different resolutions (from 30 arc minutes to 30 arc seconds) which are freely available on the Internet [1]. NCGIA also provides a list of freeware and shareware programs to handle different formats of DTM files. DTMs can be used for numerous applications such as, e.g.,

- Calculating cut-and-fill requirements for earth works engineering, such as road construction or the area that would be flooded by a hydroelectric dam.
- Analyzing intervisibility to plan route location of radar antennas or microwave towers, and to define viewsheds.
- Displaying 3D landforms for military purposes and for landscape design and planning.
- Analyzing and comparing different kinds of terrain.

V.N. Alexandrov et al. (Eds.): ICCS 2001, LNCS 2074, pp. 3–12, 2001.

- Computing slope maps, aspect maps and slope profiles that can be used to prepare shaded relief maps, assist geomorphological studies, or estimate erosion or run-off.
- Computing of geophysical terrain corrections for gravity and other field observations.
- Displaying thematic information or for combining relief data such as soils, land use or vegetation.
- Providing data for image simulation models of landscapes and geographical processes.
- Investigating of erosion processes, land slides, contamination by dangerous chemicals, etc.

Traditionally, photogrammetry has been used as the main method of producing DTMs, however, there are cases for which no aerial photography is available. Recently, with the rapid improvement in remote sensing technology, automated analysis of stereo satellite data has been used to derive DTM data. Automatic generation of elevation data from SPOT stereo satellite imagery has been discussed in [2], [3], and [4]. But even in this case, there are some places that due to some reasons such as cloud coverage, technical and/or political limitations are not covered by stereo satellite imagery.

On the other hand, the availability of single satellite imagery for nearly all of the Earth is taken for granted nowadays. But unfortunately, reconstruction of objects from monocular images is very difficult, and in some cases, not possible at all. Inverse rendering or the procedure of recovering three-dimensional surfaces of unknown objects from two-dimensional images is an important task in computer vision research. A robust procedure, which can correctly reconstruct surfaces of an object, is important in various applications such as visual inspection, autonomous land vehicle navigation, and surveillance and robot control. In the past two decades, there have been extensive studies of this topic. Shape from defocusing [5], [6], shape from stereopsis [7], shape from motion [8], shape from texture (SFT) [9], [10], and shape from shading (SFS) [11] [12], [13] are examples of techniques used for inverse rendering.

This paper is the result of investigating the use of shape from shading techniques to improve the quality of the interpolated DTM data with single satellite imagery of better resolution than the DTM data. The idea is highly motivated by the wide availability of satellite remotely sensed imagery such as Landsat TM and SPOT HRV imagery.

2 Shape from Shading

Shape recovery in computer vision is an inverse problem which transforms single or stereo 2D images to a 3D scene. Shape from stereo, shape from motion, shape from texture, and shape from shading are examples of methods used for shape recovery in computer vision. Shape from shading (SFS) recovers the surface shape from gradual variations of shading in the image. The recovered shape can be expressed either in

terrain height z(x,y) or surface normal $\vec{N}$ or surface gradient (p,q)= $(\partial z/\partial x, \partial z/\partial y)$.

To solve the SFS problem, the first step is to study the image formation process. A Lambertian model is the simplest one in which it is assumed that the gray level at each pixel depends on light source direction and surface normal. Assuming that the surface is illuminated by a distant point source, we have the following equation for the image intensity:

$$R(x,y) = \rho\ \vec{N}.\vec{L} = \rho \frac{pl_1 + ql_2 + l_3}{\sqrt{p^2 + q^2 + 1}} \quad \textbf{(1)}$$

where ρ is the surface albedo, $\vec{N}$ is the normal to the surface and $\vec{L} = (l_1, l_2, l_3)$ is the light source direction. Even if ρ and $\vec{\mathrm{L}}$ are known, the SFS problem will still be a challenging subject, as this is one nonlinear equation with two unknowns for each pixel in the image. Therefore, SFS is an underdetermined problem in nature and in order to get a unique solution, if there is any at all, we need to have some constraints.

Based on the conceptual differences in the algorithms, there are three different strategies to solve the SFS problem: 1. Minimization approaches 2. Propagation approaches, and 3. Local approaches. The following subsections briefly review these approaches. A more detailed survey of SFS methods can be found in [14].

2.1 Minimization Approaches

Based on one of the earliest minimization methods, the SFS problem is formulated as a function of surface gradients, while brightness and smoothness constraints are added to overcome the underdeterminedness condition [15]. The brightness constraint ensures the reconstructed shape produce the same brightness as the input image. The smoothness constraint in terms of second order surface gradients helps in reconstruction of a smooth surface. The shape at the occluding boundary was used for initialization to imply a correct convergence [15].

Other minimization approaches use more or less the same logic to deal with the SFS problem. However, some variations in either formulation of the problem or the constraints (or both) are usually implemented.

2.2 Propagation Approaches

In this approach there is a characteristic strip along which one can compute the surface height (object depth) and gradient, provided these quantities are known at the starting point of the strip. Singular points where the intensity is either maximum or minimum are usually the starting points. At singular points the shape of the surface is

either known or can uniquely be determined. The first attempt for solving SFS problems using this method seems to be mentioned in Horn [16]. In this technique, shape information is propagated outward along the characteristic strips. The direction of characteristic strips is toward the intensity gradient.

2.3 Local Approaches

The basic assumption in this approach is that the surface is locally spherical at each pixel point. Intensity and its first and second derivatives [17] or intensity and only its first derivative [18] have been used to estimates the shape information. All local methods suffer from the local spherical assumption which may not be correct in all cases.

Another local approach uses linearized approximations of reflectance maps to solve the SFS problem [19]. In this method the reflectance map is formulated in terms of surface gradient and then the Fourier Transform is applied to the linear function and a closed form solution for the height (depth) at each point is obtained.

Another method makes use of computing the discrete approximation of the gradient [20]. Then the linear approximation of reflectance map as a function of height (depth) is employed. Using a Jacobi iterative scheme, this technique can estimate the height (depth) at each point. The main problem of the two latter approaches is with the linear approximation of the reflectance map. If the nonlinear terms are large, it will diverge.

3 Improvement of DTM Interpolation Using SFS Techniques

The problem under investigation is to improve the accuracy of the interpolated DTM grid data by applying SFS techniques on the corresponding single satellite imagery. The assumption is that the satellite imagery has better resolution than the original DTM data. To keep the problem simple, the resolution difference between the original DTM grid data and satellite imagery is considered to be one dyadic order. The original DTM data are used as boundary constraints in the SFS problem.

The assumptions made for this research are: 1) the surface is Lambertian, 2) the surface albedo is known, 3) the surface is illuminated by a distant point source, and finally 4) the position of the light source is known.

It is worth mentioning that in our special application of SFS where we are dealing with satellite imageries, the first assumption is the only one which is questionable. However, dealing with multispectral satellite imagery, one can get a good estimate of surface albedo by applying classification techniques. Meanwhile, the light source for satellite imageries is the Sun which is not only far away from the scene, but also has a known direction knowing the local time when the satellite is passing over the scene (which is assumed to be the case).

Our approach deals with a patch located at pixel (i,j) (see Figure 1) with nine points at a time out of which there are four grid points with known heights (squares) and five unknown points (circles) for which we want to improve the accuracy of the interpolation. The method mainly consists of three stages: 1) preprocessing, 2)

processing, and 3) postprocessing. The preprocessing stage itself has two steps. In the first step, using interpolation (bilinear) techniques, the heights of the unknown points in the patch are estimated.

In the second step, using the known grid points, the relative orientation of the patch with respect to the light source is estimated. If this relative orientation implies that the patch is in the shadow, then there would be no useful shading information to improve the accuracy of the interpolated heights. Therefore, in this case the interpolated heights are considered the final height values.

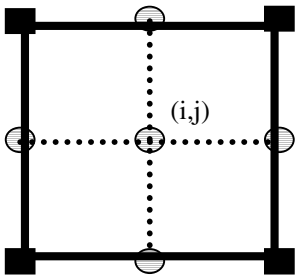

Fig. 1. A patch: squares are known grid points and circles are interpolated points.

Otherwise, the processing stage for each patch consists in solving an overdetermined system of equations of type (1) in terms of heights (z).

This is simply done by approximating p and q with finite differences. Writing the Lambertian reflectance model as a function of heights (z), we have nine nonlinear equations corresponding to the image intensity (I) of each point in the patch with four known heights (the grid points) and five unknown heights.

The nonlinear system of equations is solved using nonlinear least squares with the interpolated heights as the first approximation for the unknowns. Again it is worth mentioning that in most engineering applications, the DTM grid spacing is based on terrain roughness analysis, therefore, the interpolated heights are usually good estimates of heights for initializing the nonlinear solution. Moreover, the nonlinear least squares solution was constrained by the $\pm 3\sigma$ condition where σ is the expected standard deviation of the interpolated heights and comes from the DTM specifications.

The last stage, postprocessing, consists of taking arithmetic means of two solutions for the unknown heights located on the boundary of patches coming from the neighboring patches, except for the outsides of the peripheral patches.

4 Numerical Examples

The methodology described in Section 3 has been tested using a number of numerical examples. One synthetic object and one real DTM data set with their corresponding synthetic imageries were used in these experiments. The orientation of the light source was considered as a variable to investigate the effects of relative positions of the object and the light source on the solution.

The synthetic object under investigation is a convex hemisphere with a radius of 6 units, sampled at each 0.5 unit, i.e., a 33 by 33 pixel object. The corresponding DTM (one dyadic order less than the object, i.e., 17 by 17 pixels)) was extracted out from the object. Meanwhile, the corresponding image of the object was created using Lambertian reflectance model with a much (5 times) denser version of the object. The resulting image was passed through a smoothing filter to get an image with the same density as the original object under study.

The differences between the original object, the Interpolated Grid Solution (IGS) and the SFS solution were analyzed. Table 1 summarizes these results. The statistics shown in this table are computed with those pixels which our SFS method was able to updated their height values. The last row of the table shows the number of patches which couldn't be updated by this SFS method. This can be mainly due to two reasons. Either the patches are located with respect to the light source such that the average intensity of the patch is zero (patches in the shadow), or the nonlinear least squares process didn't converge. In Table 1 nothing has been mentioned about the azimuth of the light source. The symmetry of the synthetic object under investigation makes the process independent of the light source azimuth.

Table 1. The convex hemishpere

Elevation		30°	35°	40°	45°	50°	55°	60°
Object–IGS	Mean	-0.04	-0.04	-0.01	-0.01	0.00	-0.02	0.01
	Std	0.31	0.29	0.28	0.28	0.31	0.35	0.33
Object – SFS	Mean	-0.05	-0.07	-0.06	-0.05	-0.05	-0.06	-0.03
	Std	0.18	0.20	0.18	0.17	0.17	0.23	0.17
Patches not updated (out of 196)		41	39	28	26	19	15	20

Table 1 shows that in comparison to the IGS, the SFS solution has slightly worsened the mean differences. A detailed examination of the problem showed that this deterioration comes from the abrupt change of height values along the base of the hemisphere. Apart from these sections, the SFS solution has been able to improve the mean differences by an average of 30%. However, the improvement in the standard deviations of the differences is approximately 40% which is quite considerable. Meanwhile, for this synthetic object it is seen that the optimum elevation angle of the light source is about 50 degrees where we have about 45% improvement in standard deviation. As an example, Figure (2) shows the wiremesh of the object, the corresponding image and the wiremesh of differences of the original object and IGS,

and the SFS solution where the light source is located at azimuth and elevation angle of 135° and 45° respectively.

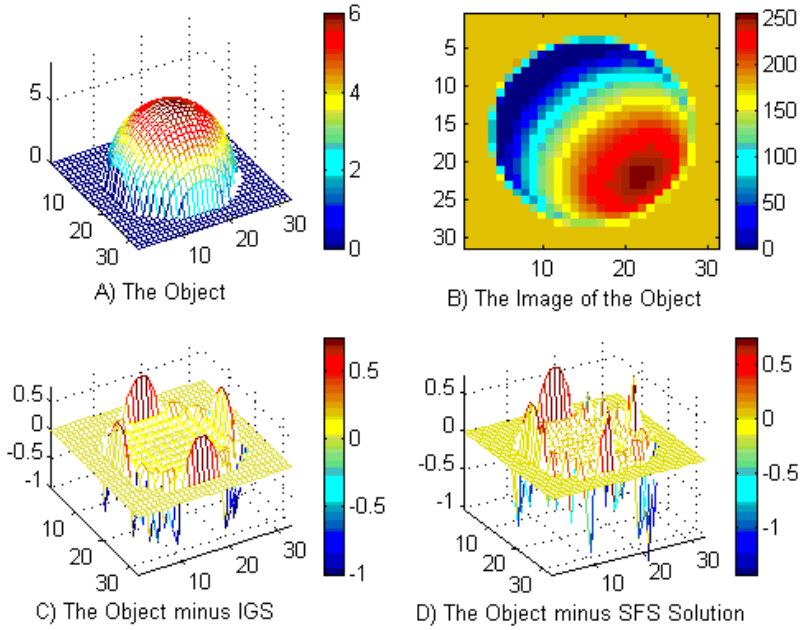

Fig. 2. A) The Original object; B) The corresponding image; The differences between the original object and the IGS in (C) and the SFS solution in (D).

The second test object is a real height data set from southern Alberta, Canada, measured with 25 metre spacing. It is a 1000 by 1000 grid with more than 1300 metre height difference which was down sampled to 125 metres (i.e., a 200 by 200 grid). This sampled height data was considered as the object under investigation and the corresponding DTM (one dyadic order wider, i.e., 250 metre grid) was extracted out from it. Meanwhile, the corresponding image of the object was created using a Lambertian reflectance model and the original 25 metre height data. The resulting image was passed through a smoothing filter to get an image with the same resolution as the object under study, i.e., 125 metres.

Table 2 summarizes the results of our experiment with this data set, which shows results similar to the previous case. The SFS solution has slightly worsened the absolute value of the mean differences and has improved the standard deviation of the mean differences with the average amount of 40%. It seems that during the data preparation process the original characteristics of the real data set has been lost. However, the results show a clear dependency of the SFS solution to the relative position of the object and the light source. As it can be seen, the worst results have been obtained with the light source at the azimuth of 180 degrees. Figure (3) shows

the wiremesh of the object, the corresponding image and the wiremesh of differences between the original object, IGS, and the SFS solution, where the light source is located at azimuth and elevation angle of 135° and 45° respectively.

Table 2. The real height data set

Azimuth		135°			180°			225°		
Elevation		30°	45°	60°	30°	45°	60°	30°	45°	60°
Object - IGS	Mean (m)	-0.01	0.09	0.22	0.71	0.41	-0.03	0.08	0.17	0.09
	Std (m)	12.9	13.2	13.6	14.4	17.2	18.8	12.8	12.9	13.4
Object - SFS	Mean (m)	0.15	-0.04	0.03	0.26	0.34	0.05	0.13	0.13	0.12
	Std (m)	7.5	7.7	7.9	8.7	10.1	11.5	7.7	7.6	7.9
Patches not updated (out of 9409)		483	872	1484	4397	3922	3709	493	735	1239

5 Remarks and Conclusions

The use of a SFS technique to improve the accuracy of the interpolated DTMs has been investigated and preliminary results are very encouraging with simulated imageries. The next step is obviously to experiment with real satellite imageries. Georeferencing, clouds, shadowing, unknown surface albedo, and noise in addition to non dyadic scale factors between satellite imageries and DTMs seem to be problems that one has to deal with before solving the SFS problem.

This SFS method is a local method that can be easily implemented by parallel processing techniques. Considering the resolution of satellite imageries and the area that they cover, one can see that using local SFS techniques and parallel processing in our application is a must.

Looking at the results, one also realizes that the success of this SFS technique is highly dependent on the relative orientation of the patches and the light source. If the

relative orientations of the object and the light source are such that there is no shading information, the SFS technique cannot improve the interpolation results. Obviously, one should not forget the morphology of the terrain. This may be another good criterion in addition to the resolution of the images, to be taken into consideration when one has different options in selecting satellite imagery for the DTM densification purposes.

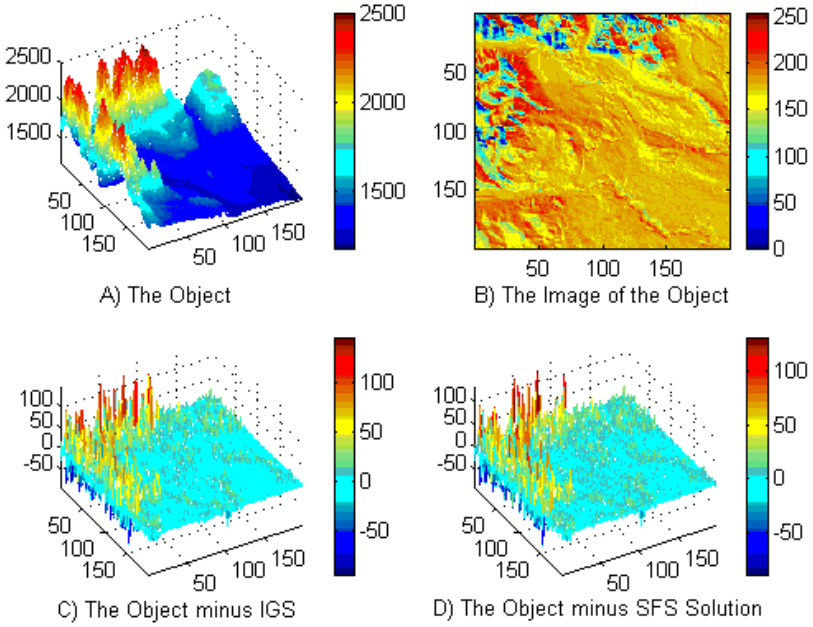

Fig. 3. A) The Original object; B) The corresponding image; The differences between the original object and the IGS in (C) and the SFS solution in (D).

References

1. The National Center for Geographic Information and Analysis (NCGIA): **www.ncgia.ucsb.edu/education/curricula/cctp/units**
2. Gugan, D. J., Dowman, I. J.: Topographic Mapping from Spot Imagery. Photgrammetric Engineering and Remote Sensing 54(10) (1988):1409-1414
3. Simard, R., Rochon, G., Leclerc, A.: Mapping with SPOT Imagery and Integrated Data Sets. Invited paper presented at the 16th congress of the International Society for Photogrammetry and Remote Sensing held July 1988 in Kyoto, Japan

4. Tam, A. P.: Terrain Information Extraction from Digital SPOT Satellite Imagery. Dept. of Geomatics Eng., The University of Calgary (1990)
5. Pentland, A. P.: A new sense for depth of field. IEEE. Trans. Pattern Anal. Match. Intell. PAMI-9(4) (1987), 523-531
6. Hwang T., Clark, J. J., Yuille, A. L.: A depth recovery algorithm using defocus information. IEEE Conference on computer vision and pattern recognition (1989), pp. 476-481
7. Medioni, J., Nevatia, R.: Segment-based stereo matching. comput. Vision Graphics Image Process, 31 July (1985), 2-18
8. Waxman, A. M., Gurumoothy, K.: Image flow theory: a framework for 3-D inference from time-varying imagery. Advances in Machine Vision (C Brown, Ed) (1988), pp. 165-224, Springer-Verlag, New York
9. Witkin, A. P.: Recovering surface shape and orientation from texture, Artif. Intell. 17 (1981), 17-47
10. Kender, J. R.: Shape from texture. Proceedings, 6th International Journal Conference on Aritficial Intelligence, Tokyo (1979), pp. 562-570
11. Wei, G.-Q., Hirzinger, G.: Parametric Shape-from-Shading by Radial Basis Functions. IEEE Transactions on Pattern Analysis and Machine Intelligence, Vol 19, No. 4, April (1997)
12. Horn, B. K. P.: Height and gradient from shading. Int. J. Comput. Vision, 37-5 (1990)
13. Zhang, R., Tsai, P. S., Cryer, J. E., Shah, M.: Analysis of Shape from Shading Techniques. Proc. Computer Vision Pttern Recognition (1994), pp. 377-384
14. Zhang, R., Tsai, P.-S., Cryer, J. E., Shah, M.: Shape from Shading: A Survey. IEEE Transcation on Pattern Analysis and Machine Intelligence, Vol. 21, No. 8, August (1999), pp. 690-706
15. Ikeuchi, K., Horn, B. K. P.: Numerical Shape from Shading and Occluding Boundaries. Artificial Intelligence, Vol. 17, Nos. 1-3 (1981), pp. 141-184
16. Horn, B. K. P.: Shape from Shading: A method for Obtaining the Shape of a Smooth Opaque from One View. PhD Thesis, Massachusetts Ins. of Technology (1970)
17. Pentland, A. P.: Local Shading Analysis, IEEE Trans. Pattern Analysis and Machine Intelligence Vol. 6 (1984), pp. 170-187
18. Lee, C. H., Rosenfeld, A.: Improved Methods of Estimating Shape from Shading Using the Light Source Coordinate System. Artificial Intelligence, Vol. 26 (1985), pp. 125-143
19. Pentland, A.: Shape information from Shading: A theory about Human Preception. Proc. Int'l Conf. Computer Vision (1988), pp. 404-413
20. Tsai, P. S., Shah, M.: Shape from Shading Using Linear Approximation, Image and Vision Computing J., Vol 12, No. 8 (1994), pp. 487-498